Mon. Not. R. astr. Soc. (1971) **151**, 161–176.

A STUDY OF α VIRGINIS WITH AN INTENSITY INTERFEROMETER

D. Herbison-Evans, R. Hanbury Brown, J. Davis and L. R. Allen

(Received 28 August 1970)

SUMMARY

Observations of the spectroscopic binary α Vir have been made with the Narrabri stellar intensity interferometer in 1966 and 1970. It has been shown that from interferometric observations alone it is possible to find the angular diameter of the primary, the brightness ratio of the components of the binary, the angular size of the semi-major axis of the relative orbit, the eccentricity, the time of periastron passage, the longitude of the line of apsides, the inclination of the orbit, the position angle of the line of nodes, the period of the orbit and the sense of the orbital motion. For α Vir, spectroscopic observations give values for four of these parameters of higher accuracy than can be obtained from the present interferometric data. Therefore, in the final analysis, these parameters were fixed at their spectroscopic values. The results for the two series of observations are in good agreement and where a spectroscopic parameter could be determined independently from the interferometric observations the agreement with the spectroscopic value is good. Interferometric and spectroscopic results have been combined to obtain the distance of α Vir (84 ± 4 pc) independent of interstellar extinction and luminosity criteria, the masses of the primary and secondary components, and the radius and surface gravity of the primary. The addition of photometric data has enabled the absolute emergent surface flux from the primary at $1{\cdot}83\,\mu^{-1}$ to be determined and, by comparing this surface flux with the predictions of theoretical model stellar atmospheres, the effective temperature of the primary has been estimated. Finally the luminosity of the primary and the absolute magnitudes of both components have been found.

1. INTRODUCTION

The stellar intensity interferometer at Narrabri Observatory has been used primarily to measure the angular diameters of single hot stars. Descriptions of the instrument (1), the technique (2) and some of the first results on single stars (3) have already been published. Recently we have started to explore the application of the instrument to more complex problems and, as part of this programme, we have observed the binary stars γ^2 Vel and α Vir. The results on γ^2 Vel have already been published (4) and the present paper reports the results on α Vir.

The first proposal that an interferometer should be used to observe binary stars was made by Michelson (5) in 1890. Subsequently, some interesting observations were carried out by Anderson (6) and by Merrill (7) who successfully measured many of the principal parameters of the double star α Aur. In principle, observations with an interferometer, made at suitable baselines and times, give the angular diameters and brightness ratio of the components of a binary and their angular separation as a function of time. From this information alone it is possible to find the angular size of the semi-major axis of the relative orbit, the eccentricity, the time of periastron passage, the longitude of the line of apsides, the inclination of the orbit, the position angle of the line of nodes, the period of the orbit and the sense of the orbital motion.

If these data from an interferometer are combined with conventional photometric and spectroscopic observations, then it is possible, again in principle, to find the distance, absolute magnitude, mass, radius, surface gravity and temperature of both the stars.

Our observations of γ^2 Vel (4) were designed primarily to find the absolute magnitude and temperature of the Wolf–Rayet component and the size of the emission region around it; neither the interferometric nor the spectroscopic data were adequate to find all the parameters of the orbit and, in particular, no attempt was made to find the inclination. In the observations reported here we have chosen to observe a well-known, double-lined, non-eclipsing spectroscopic binary (α Vir) for which adequate photometric and spectroscopic data exist, and we have sought to demonstrate how the principal parameters can be found.

2. SPECTROSCOPIC OBSERVATIONS

Spectroscopic observations of α Vir have been made since 1876 and a brief review of the principal results is to be found in the papers by Struve and his collaborators. For our present analysis we have used the observations by Struve & Ebbighausen (8) in 1933 and 1934, and by Struve *et al.* (9) in 1956, 1957 and 1958. The observed velocities for the primary and secondary, excluding all observations which are marked as affected by blending of lines, were compared in a computer with values derived from a theoretical model and the sum of the squares of the residuals (observed minus computed) was minimized to find the optimum parameters of the orbit. The theoretical model allowed different mean velocities (γ_1, γ_2) for the two stars and also allowed for a uniform rotation of the line of apsides. The minimization of the residuals and the estimate of the uncertainties in the parameters of the orbit were carried out by the same procedure as described in Section 3.2. The results are shown in Table I. It is important to note that the uncertainties shown in the Table are statistical and make no allowance for any systematic errors in the spectroscopic results.

A comparison of these results with the weighted means of the orbital elements published by Struve *et al.* (9) for 1933 and 1956 shows satisfactory agreement.

TABLE I

An analysis of the spectroscopic data for α Virginis

Parameter	Value
γ_1	$-5\cdot8 \pm 1\cdot3$ km s^{-1}
γ_2	$+8\cdot8 \pm 2\cdot1$ km s^{-1}
K_1	$123\cdot9 \pm 1\cdot4$ km s^{-1}
K_2	$198\cdot8 \pm 1\cdot5$ km s^{-1}
ω	$98 \pm 6°$ at JD 2435564
T	JD $2435563\cdot55 \pm 0\cdot07$
P	$4\cdot014550 \pm 0\cdot000032$ days
e	$0\cdot146 \pm 0\cdot009$
U	124 ± 11 yr

Furthermore, the orbital elements in Table I predict correctly the epochs of minimum velocity observed by Vogel (**10**) in 1890, by Baker (**11**) in 1908 and by Struve and Ebbighausen (**8**) in 1930.

We note that a recent investigation which has included new spectral data as well as the observations of Struve and his colleagues has led to the conclusion that there is no significant difference between γ_1 and γ_2 for α Vir. This investigation yielded mean values for the remaining parameters in Table I in satisfactory agreement with the values adopted here (N. Lomb and R. R. Shobbrook, private communication).

3. INTERFEROMETRIC OBSERVATIONS

Two series of observations of α Vir have been made with the stellar intensity interferometer at Narrabri. The first series was made in 1966. A method of analysing the results was developed and the final analysis completed in 1970. A second series of observations was made in 1970.

3.1 *Method of observation*

The observations were all carried out using our standard observing procedure which has been described in a previous paper (**1**). Briefly the two reflectors of the interferometer are guided to follow the star and their separation, the baseline, is maintained constant and perpendicular to the direction of the star. The correlation is measured over intervals of 100 s and recorded together with the light fluxes received by the two reflectors. The observed correlation is then normalized by the light fluxes and by the gain of the electronic equipment to find the *normalized observed correlation* $\overline{c_N(d)}$ for each interval. Typically these observations are continued for several hours at one baseline and then repeated at other baselines.

3.2 *Method of analysis*

A computer program was written to calculate the correlation expected from a binary star as a function of time for a given set of orbital parameters. The component stars were assumed to present uniformly bright circular discs. Under these conditions the normalized correlation $\overline{c_N(d)}$ is given by

$$\overline{c_N(d)} = \frac{A}{(1+\beta)^2}\left[\beta^2\Gamma_1{}^2(d)+\Gamma_2{}^2(d)+2\beta|\Gamma_1(d)|\,|\Gamma_2(d)|\cos\left(\frac{2\pi\theta_s\, d\cos\psi}{\lambda_0}\right)\right] \quad (1)$$

where

$$\Gamma_1(d) = \frac{2J_1(\pi\theta_{UD1}\, d/\lambda_0)}{\pi\theta_{UD1}\, d/\lambda_0}$$

$$\Gamma_2(d) = \frac{2J_1(\pi\theta_{UD2}\, d/\lambda_0)}{\pi\theta_{UD2}\, d/\lambda_0}$$

and λ_0 is the wavelength of observation; θ_{UD1} and θ_{UD2} are the angular diameters (equivalent uniform discs) of the primary and secondary; β is the brightness ratio of the components ($\beta \geqslant 1$); θ_s is the angular separation of the components projected on to the plane of the sky; ψ is the angle in the plane of the sky between the projection of the line joining the stars and the baseline of the interferometer; A is an instrumental constant, which, in effect, is the normalized correlation to be expected from an unresolved single star. The parameters of the orbit which enter the calculation are, θ_a the angular semi-major axis, i the inclination of the orbital plane, Ω the position angle of the line of nodes, e the eccentricity, T the epoch of periastron passage, ω the longitude of the line of apsides, P the period of the orbit measured from periastron to periastron, and U the period of rotation of the line of apsides. The sense of rotation of the stars in their orbit and of the line of apsides also enter the calculation.

As a first step in the analysis the values of T, e, P, ω, U and θ_{UD2} were fixed in the computer at the values shown in Table I, leaving six free parameters, i, θ_a, β, Ω, θ_{UD1} and A to be found by comparing the observed and computed correlations. As we shall see later the spectroscopic values of T, e, P and ω are superior in accuracy to those which can be found from the interferometer and, as we expected, the signal/noise ratio of the observations was inadequate to find the value of θ_{UD2} with acceptable accuracy. The ' fixed ' values of T, e, P and ω were therefore taken from the spectroscopic data in Table I and the value of θ_{UD2} was estimated with the aid of a preliminary analysis. It was also assumed that the period of rotation of the line of apsides was infinite over the period of observation and hence $U = \infty$ and ω has fixed values appropriate to the mean epochs of observation in 1966 and 1970. Initial values for the ' free ' parameters, as a starting point for the programme, were taken from a preliminary analysis (**12**) and the normalized correlation was computed for each of the intervals of observation.

The calculation was performed as follows: for each interval of Julian date J, the mean anomaly m was computed from

$$m = 2\pi(J-T)/P \tag{2}$$

then the eccentric anomaly E from the first order approximation

$$E = m+\frac{e \sin m}{1-e \cos m} \tag{3}$$

then the true anomaly v from

$$\tan\left(\frac{v}{2}\right) = [(1+e)/(1-e)]^{1/2} \tan\frac{E}{2} \tag{4}$$

and the angular separation of the stars θ_r from

$$\theta_r = \theta_a(1-e^2)/(1+e \cos v) \tag{5}$$

and hence the projected angular separation of the stars in the plane of the sky θ_s was found from

$$\theta_s = \theta_r[1-(\sin i . \sin \overline{\omega+v})^2]^{1/2}. \tag{6}$$

The position angle ψ of the line joining the stars, relative to the baseline of the interferometer, was computed from

$$\psi = \Omega+\frac{\pi}{2}+\eta+\delta_1\delta_2 \cos^{-1}\left[\frac{\cos \overline{\omega+v}}{(1-\sin^2 i . \sin^2 \overline{\omega+v})^{1/2}}\right] \tag{7}$$

where δ_1 is -1 for a clockwise and $+1$ for an anti-clockwise orbit, and δ_2 is $+1$ for $0<\omega+v<180°$ and -1 for $180°<\omega+v<360°$, and the solution to the $\cos^{-1}$ term is chosen to lie between 0 and π. The parallactic angle η is the angle at the star, in the sky plane, between the vertical circle and the great circle through the star and the poles. η is given by

$$\sin \eta = \cos \phi \sin H / \sin Z \tag{8}$$

where ϕ is the latitude, H is the hour angle and Z is the zenith distance. Finally the values of θ_s and ψ from equations (6) and (7) were substituted in equation (1) to calculate the correlation (c_c) for each interval.

The difference between the observed and the calculated correlation $(\overline{c_N(d)} - c_c)$ was then found for each interval, squared, and weighted by the square of the corresponding 'signal/noise ratio'. It can be shown (**1**) that this signal/noise ratio is proportional to $(I_1 I_2)^{1/2}$ where I_1, I_2 are the light fluxes received by the two reflectors in the interval. The square root of the mean value of the weighted, squared differences is the r.m.s. residual σ_r so that

$$\sigma_r = \left[\sum_M (\overline{c_N(d)} - c_c)_i^2 (I_1 I_2)_i / M \right]^{1/2} \tag{9}$$

where M is the number of intervals observed. The value of σ_r was then minimized by optimizing the 'free' input parameters of the theoretical model using an iterative programme based on the Simplex Method (**13**).

The uncertainty in the optimized free parameters was found by computing the partial derivatives of the theoretical correlation with respect to each parameter at the time of each observation. These derivatives were then weighted in proportion to the signal/noise ratio by $(I_1 I_2)^{1/2}$, and the resulting matrix of weighted derivatives was multiplied by its transpose, and inverted. The square root of the pth diagonal element of this inverse (x_{pp}) was then multiplied by the r.m.s. residual σ_r to find the r.m.s. uncertainty σ_p in the pth free parameter, where

$$\sigma_p = \sigma_r \sqrt{x_{pp}}. \tag{10}$$

The whole analysis was carried out twice, for clockwise and anti-clockwise orbital motion. Although these two cases cannot be distinguished spectroscopically they can be distinguished by the interferometer, given sufficient observations of high signal/noise ratio, because the orbital motion adds to or subtracts from the parallactic angle.

3.3 *Observations in* 1966

α Vir was observed for 12 nights in May 1966 with baselines of 10·0, 32·7, 59·7 and 88·3 m for a total time of about 84 hr. The effective wavelength was 4430 Å with a total filter bandwidth of 100 Å. To reduce the amount of computing the normalized correlations at each baseline were averaged over 25 intervals of 100 s to find the normalized observed correlation for periods of 2500 s. The results were then compared with calculated values in the computer to find the optimum values of the six 'free' parameters and their associated uncertainties. A unique minimum in the residual σ_r was found for both choices of the sense of orbital motion and the results are shown in columns 4 and 5 of Table II. The expected value of the residual σ_r is σ_{std}, the normalized r.m.s. uncertainty due to noise in the correlator output (**3**). We have, therefore, shown σ_r/σ_{std} in Table II, taking values of σ_{std} measured independently for the configuration of the apparatus in 1966.

Table II shows that although the values of Ω and i are significantly different for the two solutions, the residuals σ_r are not. The values of σ_r are both consistent with

11

1971MNRAS.151..161H

Table II

Analysis of interferometric observations

(1) Parameter	(2) Symbol	(3) Units	(4) 1966	(5) 1966	(6) 1970	(7) 1970	(8) 1970	(9) 1970	(10) 1970 (Final analysis)
Number of free parameters			6	6	6	6	11	11	6
Inclination of orbit	i	degrees	63 ± 4	76 ± 3	65 ± 2	90 ± 4	65 ± 2	90 ± 4	65·9 ± 1·8
Angular size of primary	θ_{UD1}	10^{-3} arc sec	0·76 ± 0·06	0·74 ± 0·06	0·87 ± 0·04	0·97 ± 0·08	0·88 ± 0·04	0·93 ± 0·05	0·87 ± 0·04
Angular size of secondary	θ_{UD2}	10^{-3} arc sec	(0·4)	(0·4)	(0·4)	(0·4)	~0	1·3 ± 0·4	(0·4)
Angular size of semi-major axis	θ_a	10^{-3} arc sec	1·42 ± 0·10	1·42 ± 0·11	1·52 ± 0·05	1·37 ± 0·09	1·52 ± 0·04	1·32 ± 0·11	1·54 ± 0·05
Brightness ratio of components	β		6·2 ± 1·9	6·2 ± 2·0	6·2 ± 0·9	8·1 ± 2·6	6·4 ± 0·9	5·5 ± 1·5	6·4 ± 1·0
Position angle of line of nodes	Ω	degrees	122 ± 5	158 ± 4	132·1 ± 2·1	142·2 ± 3·2	130·8 ± 2·0	142·2 ± 3·4	131·6 ± 2·1
Epoch of periastron passage	T	JD	(2439256·94)	(2439256·94)	(2440678·09)	(2440678·09)	2440678·02 ± 0·08	2440678·16 ± 0·35	(2440678·09)
Eccentricity of orbit	e		(0·146)	(0·146)	(0·146)	(0·146)	0·160 ± 0·021	0·139 ± 0·052	(0·146)
Longitude of line of apsides	ω	degrees	(127)	(127)	(138)	(138)	132 ± 8	150 ± 33	(138)
Inverse period	$1/P$	1/days	(0·249091)	(0·249091)	(0·249091)	(0·249091)	0·2481 ± 0·0006	0·2459 ± 0·0012	(0·249091)
Sense of orbital motion			Clockwise	Anti-clockwise	Clockwise	Anti-clockwise	Clockwise	Anti-clockwise	Clockwise
Instrumental constant	A	arbitrary	1·77 ± 0·06	1·71 ± 0·06	5·01 ± 0·18	4·65 ± 0·19	4·97 ± 0·17	4·91 ± 0·29	5·00 ± 0·19
r.m.s. residual/normalized noise	σ_r/σ_{std}		0·22/0·20	0·23/0·20	0·25/0·27	0·31/0·27	0·25/0·27	0·30/0·27	0·26/0·27
Interval over which observations were averaged		seconds	2500	2500	2500	2500	2500	2500	500
Number of intervals used			112	112	158	158	158	158	800

Notes: The values taken from spectroscopic data (Table I) are in brackets. The value of θ_{UD2} in brackets is assumed (see text).

the expected value of $\sigma_{std} = 0{\cdot}20$. Thus it appears that the signal/noise ratio of these observations is inadequate to distinguish the correct sense of orbital motion from a simple comparison of the ' goodness of fit ' of the two solutions. In addition, a more detailed examination suggests that, to solve this particular problem, our choice of baselines could have been better. Fortunately, the difference between the inclinations (i) of the two solutions shows that the clockwise solution must be correct; the high inclination (76°) of the anti-clockwise orbit implies eclipses which are not observed (see Section 4.2).

3.4 *Observations in* 1970

Following a complete analysis of our 1966 observations we decided to observe α Vir again to check the whole procedure and to increase the precision of the results. Specifically we hoped to improve the accuracy by a different choice of baselines and by taking advantage of improvements to the interferometer which had raised its signal/noise ratio by a factor of about 1·6. The most significant of these improvements was the introduction in 1969 of R.C.A. type 8850 phototubes with high-gain first dynodes.

The second series of observations was made on 16 nights in March and April 1970 with baselines of 19·7, 39·1 and 83·9 m for a total time of about 115 hr. Again the effective wavelength was 4430 Å with a total filter bandwidth of 100 Å.

Initially, the observations were analysed in precisely the same way as the 1966 series to find the six free parameters. As for the 1966 data two unique minima were found for the residual σ_r, corresponding to the two senses of orbital motion, and the results are shown in columns 6 and 7 of Table II. The values of σ_r are not inconsistent with the expected value of $\sigma_{std} = 0{\cdot}27$, measured for the configuration of the equipment used in 1970, but they do differ significantly from one another. The r.m.s. uncertainty in each value of σ_r is about $\pm 0{\cdot}02$ and so the residual for clockwise rotation (0·25) is three standard deviations less than the residual for anti-clockwise rotation (0·31), thus confirming our earlier conclusion that the clockwise solution must be correct. Furthermore, the inclination of the anti-clockwise solution ($90° \pm 4°$) is again definitely excluded by the absence of eclipses.

A comparison of columns 4 and 6 of Table II shows that the parameters derived from the 1966 and 1970 observations are in satisfactory agreement and that the 1970 results are, as expected, about twice as accurate. The largest differences are in Ω and θ_{UD1} which differ by about $1{\cdot}9\sigma$ and $1{\cdot}5\sigma$ respectively, where σ is their combined uncertainty. It must be noted that the instrumental constants A are widely different because they refer to different configurations of the equipment.

As a further check on the reliability of our results, we have tested their consistency with the spectroscopic data. This we have done by removing the spectroscopic data entirely and allowing the computer to optimize all 11 parameters of the star (θ_a, θ_{UD1}, θ_{UD2}, i, β, Ω, T, e, ω, A and P). Again two minima close to the expected period of the star were found corresponding to clockwise and anti-clockwise rotation and the results are shown in columns 8 and 9 of Table II. The two residuals σ_r differ significantly and show that the clockwise solution is correct. A comparison of the four parameters T, e, ω, and P in Table II with the spectroscopic data in Table I shows that there are no significant differences, but that the spectroscopic data are more precise. The other six parameters agree well with the values shown in columns 6 and 7 for the six ' free ' parameter analysis. The value of θ_{UD2}, the angular size of the secondary star, is undetermined because the signal/noise ratio was inadequate. However, an examination was made of the effects of changes in the assumed value of θ_{UD2}. They were found to be negligible. This can also be seen from a comparison of the solutions in which θ_{UD2} was fixed (columns 6 and 7 in Table II) with those in which it was a free parameter (columns 8 and 9). We conclude from this analysis that our interferometric results are consistent with the spectroscopic data.

Finally, we have tested the dependence of our results on the period over which the observed correlations are averaged. To this end we have averaged the observed correlations over intervals of 500 s, instead of 2500 s, and repeated the calculations shown in column 6 of Table II. Since this is an extensive calculation it has only been carried out for the correct sense of orbital motion (clockwise). For this refined calculation an attempt was made to reject any observations which might be defective. The computer program was therefore modified to reject all observations which differ by more than $2{\cdot}5\sigma_r$ from the calculated values and, as a result, 19 of the 819

Ω° \ i°	30	35	40	45	50	55	60	65	70	75	80	85
0	.635	.635	.635	.634	.632	.627	.620	.610	.598	.582	.564	.544
5	.647	.652	.656	.659	.660	.658	.653	.644	.631	.616	.597	.577
10	.652	.661	.669	.676	.681	.682	.680	.672	.661	.646	.628	.607
15	.647	.660	.672	.684	.693	.698	.699	.695	.685	.672	.655	.635
20	.634	.649	.665	.681	.694	.704	.709	.709	.703	.692	.678	.660
25	.616	.632	.650	.668	.685	.699	.708	.713	.713	.708	.698	.685
30	.598	.613	.630	.648	.667	.684	.699	.710	.717	.719	.716	.707
35	.582	.594	.609	.626	.644	.664	.683	.701	.716	.726	.729	.726
40	.572	.581	.592	.607	.624	.644	.665	.688	.710	.727	.738	.742
45	.569	.575	.584	.595	.609	.627	.649	.675	.701	.724	.742	.752
50	.573	.577	.583	.590	.601	.616	.636	.662	.690	.717	.740	.755
55	.579	.582	.586	.590	.597	.609	.627	.650	.678	.706	.731	.749
60	.585	.587	.588	.591	.597	.606	.620	.640	.664	.689	.714	.732
65	.586	.587	.589	.591	.595	.602	.612	.627	.645	.666	.687	.703
70	.583	.584	.586	.587	.590	.593	.599	.608	.620	.635	.651	.665
75	.576	.576	.576	.577	.577	.577	.579	.582	.589	.598	.608	.620
80	.563	.562	.561	.560	.558	.556	.554	.553	.553	.556	.562	.572
85	.546	.545	.544	.542	.539	.534	.528	.521	.515	.512	.515	.524
90	.527	.527	.527	.525	.521	.514	.503	.490	.478	.470	.470	.480
95	.508	.509	.510	.509	.504	.494	.478	.460	.443	.433	.432	.443
100	.488	.490	.492	.492	.486	.473	.454	.433	.414	.403	.402	.413
105	.466	.469	.470	.469	.462	.448	.428	.407	.389	.379	.380	.392
110	.442	.444	.444	.441	.433	.418	.398	.378	.364	.358	.363	.379
115	.418	.417	.414	.408	.398	.382	.362	.345	.336	.338	.350	.372
120	.398	.393	.386	.376	.362	.343	.323	.309	.307	.318	.340	.368
125	.386	.377	.366	.352	.332	.309	.287	.276	.280	.301	.331	.364
130	.385	.374	.360	.341	.316	.289	.265	.256	.265	.291	.326	.359
135	.397	.384	.368	.346	.319	.290	.267	.258	.268	.292	.324	.353
140	.419	.406	.389	.367	.340	.314	.293	.283	.288	.305	.328	.349
145	.448	.436	.419	.398	.375	.352	.333	.322	.320	.327	.339	.350
150	.481	.469	.454	.436	.416	.396	.379	.365	.358	.357	.359	.360
155	.514	.504	.490	.475	.457	.440	.423	.409	.398	.392	.387	.381
160	.545	.536	.524	.511	.496	.480	.465	.451	.440	.431	.421	.408
165	.573	.565	.555	.544	.532	.518	.505	.493	.482	.470	.457	.441
170	.597	.591	.584	.575	.566	.556	.545	.534	.523	.510	.494	.475
175	.618	.614	.610	.606	.600	.592	.584	.574	.562	.547	.529	.510
180	.635	.635	.635	.634	.632	.627	.620	.610	.598	.582	.564	.544

FIG. 1. *Map of the r.m.s. residual* (σ_r) *as a function of the position angle of the line of nodes* (Ω) *and the inclination* (i) *with the remaining nine parameters fixed at the values given in column* 10 *of Table II.*

intervals were rejected. A check was made that these rejected observations were not distributed in any systematic way. The results are shown in column 10 of Table II. We note that they are consistent with the results in column 6 of Table II and, since they represent the most exact analysis which it is worth making, we shall take them as our final results for α Vir.

Figs 1 and 2 illustrate the calculations presented above. Fig. 1 is a map of the r.m.s. residual σ_r as a function of the two parameters Ω and i, all the other parameters being fixed at their optimum values. The contours show clearly the unique minimum in σ_r corresponding to the clockwise solution presented in column 6 of Table II. It is fortuitous that in the case of α Vir the orbital period (4·014 days) is so close to 4 days that, over the observation period of 20 days, the binary system presents essentially the same phase every fourth night. In Fig. 2 we have plotted the correlation as a function of hour angle for 12 nights divided into 4 sets; each set is the average of the

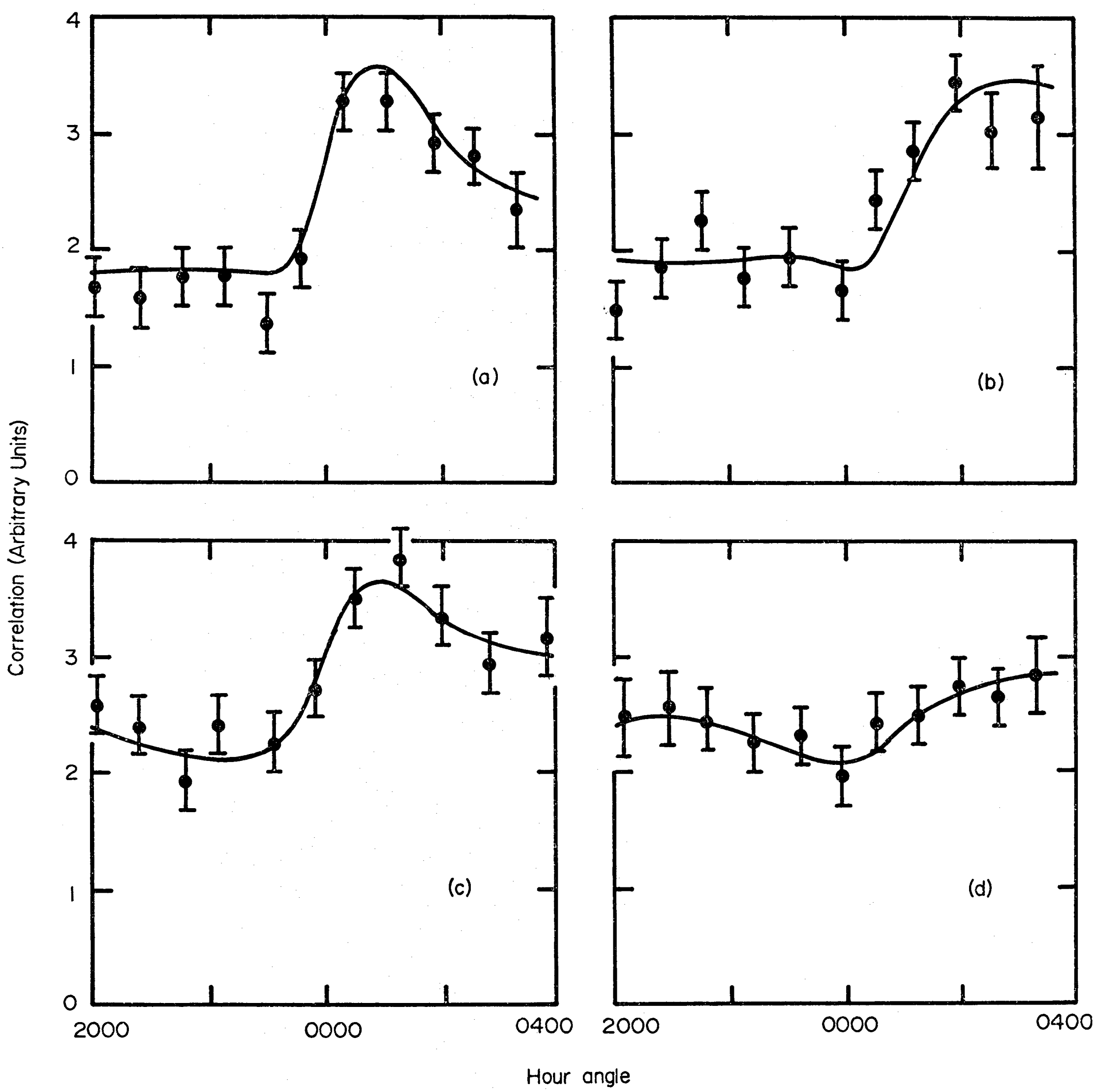

FIG. 2. *Variation of correlation from α Vir observed in* 1970 *with a baseline of* 39·1 *m for four different 'phases' (see text). Observations for the four 'phases' were combined for the Julian Days of observation as follows*: (*a*) *JD*2440672, 680 *and* 692. (*b*) *JD*2440673, 677 and 689. (*c*) *JD*2440678, 682 *and* 690. (*d*) *JD*2440675, 683 and 691.

The curves represent the average computed correlation for the periods of observation using the parameters of the solution given in column 10 *of Table II.*

correlation on 3 nights which are themselves separated by either 4 or 8 days. The points show the average of the correlation observed on the 3 nights in 2500 s intervals, and the full line is the average of the correlation calculated for those 3 nights. The curves show clearly the variation of correlation with time for the four different phases of the system.

Detailed lists of all the observations are available and the authors will be glad to supply them to anyone who is interested. We have not included them in the present paper because they are lengthy and we judge that they are not of sufficient interest to justify the space.

3.5 *Corrections and errors*

In the analysis presented above, the uncertainties in the final parameters have been estimated on the assumption that the weighted differences between the observed and computed correlations represent random errors which are normally distributed. No allowance has been made for systematic errors. An examination of the weighted differences for the results shown in Table II confirms that they are normally distributed. Furthermore, the r.m.s. residual σ_r is, as already noted, consistent with the assumption that the principal source of uncertainty is the statistical noise in the correlator output. Nevertheless, these two tests do not exclude the possibility that there are systematic errors in our measurements. We have, therefore, reviewed all the principal sources of systematic error (timing errors, delay errors, gain calibration, sky and moon background light, non-linearity, effects of elevation, computing approximations, etc.), and have reached the conclusion that, in the present experiments, where the signal/noise ratio is rather low, the systematic errors are small compared with the statistical noise. This conclusion is reinforced by the agreement between the interferometric and spectroscopic parameters discussed in Section 3.4. We shall, therefore, proceed to discuss the results on the assumption that the 'statistical' errors shown in Table II are reasonable estimates of the uncertainties.

There are a number of minor corrections which remain to be discussed. Firstly, the theoretical model assumes that the two stars have circular discs of uniform intensity which do not vary with time. In reality the two stars will be limb-darkened, distorted by rotation and mutual interaction, and the light and radius of the primary will vary because it is a β Cepheid variable (**14**). Neglect of limb-darkening will not affect the solution for the orbital elements, but it is taken into account in Section 4.1 in finding the true angular size of the primary θ_{LD1} from the angular size of the equivalent uniform disc θ_{UD1}. We have also made estimates of the effects of rotation and tidal distortion on our results and find them to be negligible. The effects of the variations in light of the primary are, to a first order, removed by normalization and theory suggests that the associated periodic changes in radius are too small to be significant in the present context.

In principle, minor corrections should also be made for the effects of partial resolution by the reflectors. The two reflectors themselves are so large (6·5 m diameter) in relation to the baseline that they partially resolve the separation of the two stars when they appear furthest apart, thereby reducing the amplitude of the interaction term in equation (1). In widely-separated binaries this effect limits the use of an intensity interferometer (**15**), but in the present case calculations show that the only significant effect is to increase the computed value of β, the brightness ratio, by a few per cent. Since this is small compared with the uncertainty in β, no correction has been made to the data in Table II. Lastly, there is the reflection effect which brightens the inner surfaces of the components of a close binary and thereby reduces their apparent separation as seen by the interferometer. Following Chen & Rhein (**16**) we have computed the apparent increase in the brightness of the inner surfaces and find that, in the present case, the apparent shift is less than 10^{-3} of the semi-major axis. No correction for the reflection effect has therefore been applied.

4. DISCUSSION

4.1 *Combined interferometric, spectroscopic and photometric results*

The results of combining the data from interferometric, spectroscopic and photometric observations are shown in Table III.

TABLE III

The parameters of α Virginis

Parameter	Value ± r.m.s. uncertainty	Source*
Inclination of orbit (i)	$65°·9 \pm 1°·8$	I
Angular size of primary (limb-darkened) (θ_{LD_1})	$(0''·90 \pm 0''·04) \times 10^{-3}$	I
Angular size of semi-major axis (θ_a)	$(1''·54 \pm 0''·05) \times 10^{-3}$	I
Brightness ratio of components (β)	$6·4 \pm 1·0$	I
Position angle of line of nodes (Ω)	$131°·6 \pm 2°·1$	I
Sense of orbital motion	Clockwise	I
Epoch of periastron passage (T)	JD 2440678·09	S
Eccentricity of orbit (e)	0·146	S
Longitude of line of apsides (ω)	138° at JD 2440678	S
Inverse period ($1/P$)	0·249091 days^{-1}	S
Period of rotation of line of apsides (U)	124 yr	S
Semi-major axis (a)	$(1·93 \pm 0·06) \times 10^7$ km	I+S
Distance	84 ± 4 pc	I+S
Mass of primary (m_1)	$10·9 \pm 0·9\ m_\odot$	I+S
Mass of secondary (m_2)	$6·8 \pm 0·7\ m_\odot$	I+S
Radius of primary (R_1)	$8·1 \pm 0·5\ R_\odot$	I+S
Surface gravity of primary ($\log g_1$)	$3·7 \pm 0·1$ [g_1 in c.g.s. units]	I+S
Absolute surface flux of primary ($\mathscr{F}_{\nu_1}$ at $1·83\ \mu^{-1}$)	$(2·75 \pm 0·24) \times 10^{-3}$ erg cm^{-2} s^{-1} Hz^{-1}	I+P
Effective temperature of primary (T_{e_1})	22400 ± 1000 °K	I+P
Luminosity of primary ($\log L_1/L_\odot$)	$4·17 \pm 0·10$	I+S+P
Absolute magnitude of primary (M_{V_1})	$-3·5 \pm 0·1$	I+S+P
Absolute magnitude of secondary (M_{V_2})	$-1·5 \pm 0·2$	I+S+P

* I = interferometric, S = spectroscopic, P = photometric.

To find the distance of α Vir we first calculated the projected semi-major axi from K_1, K_2, P and e in Table I. From the standard relation we found

$$a \sin i = (1·76 \pm 0·05) \times 10^7 \text{ km}. \qquad (11$$

The uncertainty in this result is difficult to estimate. It was noted in Section 2 that the uncertainties in K_1, K_2 in Table I are only statistical and make no allowance for systematic errors. An examination of the difference between the results obtained by Struve and his colleagues (**9**) in 1933 and 1956, together with his comments about the blending and variability of the lines, suggests that there may be significant systematic errors in K_1 and K_2; furthermore, we now know (**14**) that the primary star is a β Cepheid which complicates the interpretation of the spectrum. We have therefore increased the uncertainties given in Table I to cover the range of Struve's results, and we have taken the uncertainty in K_1 to be ± 7 km s^{-1} and in K_2 to be ± 5 km s^{-1}. The corresponding uncertainty in $a \sin i$ is that shown in equation (11); the errors in e and P have little effect. The distance of α Vir was then calculated from the projected size of the semi-major axis ($a \sin i$ from equation (11)), the inclination of the orbit and the angular size of the semi-major axis (i and θ_a from column 10 of Table II). The resulting distance is 84 ± 4 pc where the major uncertainty is due to the spectroscopic data.

To find the masses of the components of α Vir we first calculated the values of $m_1 \sin^3 i$ and $m_2 \sin^3 i$ from the spectroscopic data. Using the standard relation and the same uncertainties in K_1 and K_2 we have

$$m_1 \sin^3 i = 8{\cdot}3 \pm 0{\cdot}6\ m_\odot$$
$$m_2 \sin^3 i = 5{\cdot}2 \pm 0{\cdot}5\ m_\odot. \tag{12}$$

The masses given in Table III were found by combining these values with i from column 10 of Table II.

The angular diameter of the primary (θ_{LD1}) was found by correcting θ_{UD1} to allow for limb-darkening. Following a previous discussion (**3**) we have taken $\theta_{LD1}/\theta_{UD1} = 1{\cdot}03$ for an assumed limb-darkening coefficient $U_{4430} = 0{\cdot}39$. The radius of the primary R_1 given in Table III was then found from θ_{LD1} and the distance, and the surface gravity from m_1 and R_1.

The effective temperature T_{e_1} of the primary was found as follows. The absolute monochromatic flux at the Earth (f_ν) from the primary, at the constant energy reciprocal wavelength ($1/\lambda_0 = 1{\cdot}83\mu^{-1}$) of the V band (**17**), was calculated from

$$f_\nu = 3{\cdot}71 \times 10^{-20} \times 10^{-0{\cdot}4V} \text{ erg cm}^{-2}\text{ s}^{-1}\text{ Hz}^{-1} \tag{13}$$

where $3{\cdot}71 \times 10^{-20}$ erg cm^{-2} s^{-1} Hz^{-1} has been adopted as the flux received above the Earth's atmosphere from a star with $V = 0{\cdot}00$, this being the mean of a new determination by Oke & Schild (**18**) and the value proposed by Davis & Webb (**19**) from a review of earlier work. The visual magnitude V of the primary was taken to be $+1{\cdot}13$ from $V = +0{\cdot}97$ for α Vir (**20**) and $\Delta V = 2{\cdot}0$ (from $\beta = 6{\cdot}4$ in Table III). Thus, for the primary, $f_\nu = 1{\cdot}31 \times 10^{-20}$ erg cm^{-2} s^{-1} Hz^{-1} at $1{\cdot}83\ \mu^{-1}$.

At this point we note that ΔV has been determined using a spectroscopic method by Struve (**21**) who obtained $\Delta V \simeq 2{\cdot}4$, Petrie (**22**) $\Delta V = 1{\cdot}49$ and Struve *et al.* (**9**) $\Delta V = 1{\cdot}69$. In view of the spread in values obtained by the spectroscopic method we have chosen to use the interferometric value of $\Delta V = 2{\cdot}0 \pm 0{\cdot}2$ throughout our discussion of the results.

The absolute monochromatic flux at the stellar surface ($\mathscr{F}_\nu$) was found next from

$$\mathscr{F}_\nu = \frac{4 f_\nu}{\theta_{LD}{}^2} \cdot 10^{0{\cdot}4 A_\nu} \tag{14}$$

where A_ν is the total interstellar absorption at frequency ν. A comparison of the observed colours of α Vir (**20**) with the intrinsic colours (**23**) for a B1·5 IV–V star with a B3V companion (see Section 4.2) suggests that E_{B-V} is small ($\sim$0·01) and we have therefore assumed α Vir to be unreddened with $A_v = 0{\cdot}00$. Substitution in equation (14) gives $\mathscr{F}_{\nu_1} = (2{\cdot}75 \pm 0{\cdot}24) \times 10^{-3}$ erg cm^{-2} s^{-1} Hz^{-1} where the uncertainty corresponds to the uncertainties in θ_{LD} and ΔV and does not include those in the absolute flux (f_ν) and interstellar extinction.

The effective temperature of the primary was estimated by comparing the empirical value of $\mathscr{F}_{\nu_1}$ with the fluxes given at $1{\cdot}83\mu^{-1}$ by the ultra-violet line-blanketed model atmospheres of Bradley & Morton (**24**) and Van Citters & Morton (**25**) for $\log g = 3{\cdot}5$ and 4·0. Note that the tabulated fluxes for the models must be multiplied by π to give the physical fluxes corresponding to the observed flux. Interpolating for $\log g = 3{\cdot}7$ we found $T_e = 22\,400 \pm 1000\,°$K for the effective temperature of the primary.

The luminosity of the primary in terms of the solar luminosity ($L_1/L_\odot$) was calculated from $R_1/R_\odot$ and $T_{e1}/T_{e_\odot}$ taking $T_{e_\odot} = 5780\,°$K (**26**).

Finally, the absolute magnitudes, M_{V_1} and M_{V_2}, of the two components were found from $V = 0{\cdot}97$ (20), $\Delta V = 2{\cdot}0 \pm 0{\cdot}2$ (β in Table III) and the distance.

4.2 *Discussion of results*

The distance (84 ± 4 pc) which we find for α Vir differs from the value of 53 pc given in the *Supplement to the General Catalogue of Trigonometrical Parallaxes* (**27**). However, this difference cannot be regarded as significant because the latter value is the weighted mean of three independent observations giving 111, 59 and 34 pc. It is important to note that our measurement of distance is based only on measurements of velocity and angle, and is therefore independent of interstellar extinction or spectroscopic criteria of luminosity.

Our results for α Vir allow us to add a new point to the few existing data in the

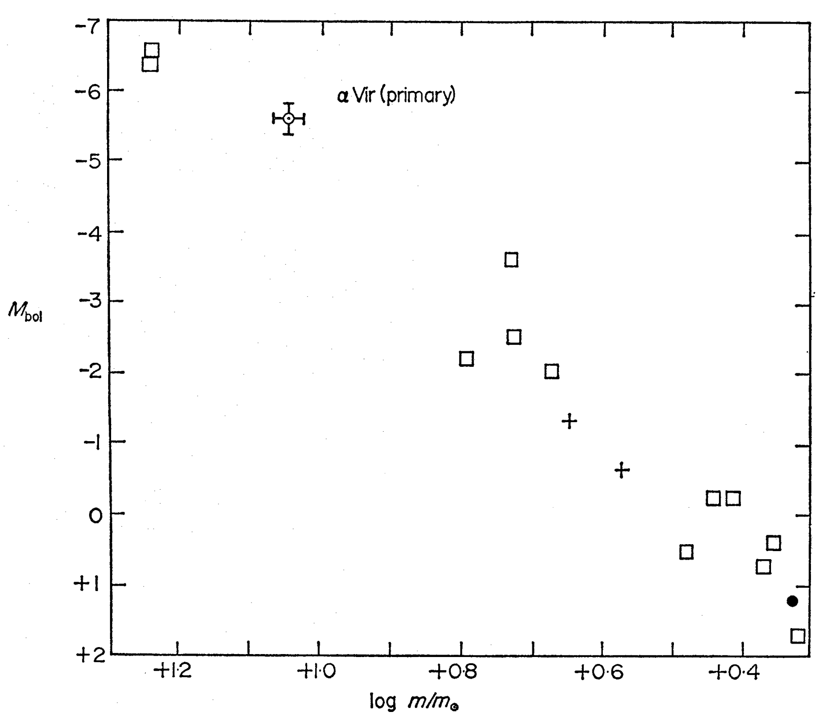

FIG. 3. *The empirical mass–luminosity relation for early-type stars.* □—*eclipsing binary data listed by Harris* et al. (**28**) *in their Table* 3; +—*CO Lac* (*Smak* (**29**)); ●—*α CMa as listed by Harris* et al. (**28**) *in their Table* 2.

mass–luminosity and mass–radius relationships for early type stars. In Figs 3 and 4 we have plotted our results for the primary together with the existing data for binary stars of spectral type A1 and earlier. The data for the mass–luminosity plot in Fig. 3 are taken from the list of Harris, Strand & Worley (**28**) for ' reliable ' spectroscopic binaries with the addition of the data for the components of CO Lac by Smak (**29**). It can be seen that the data for the primary of α Vir are consistent with other binary stars.

The mass–radius data in Fig. 4 are from the compilation by Popper (**30**) of ' reliable ' systems with the addition of the data for CO Lac (**29**). Also included is the point for the primary of αCMa (Sirius), the mass being taken from Harris *et al.* (**28**)

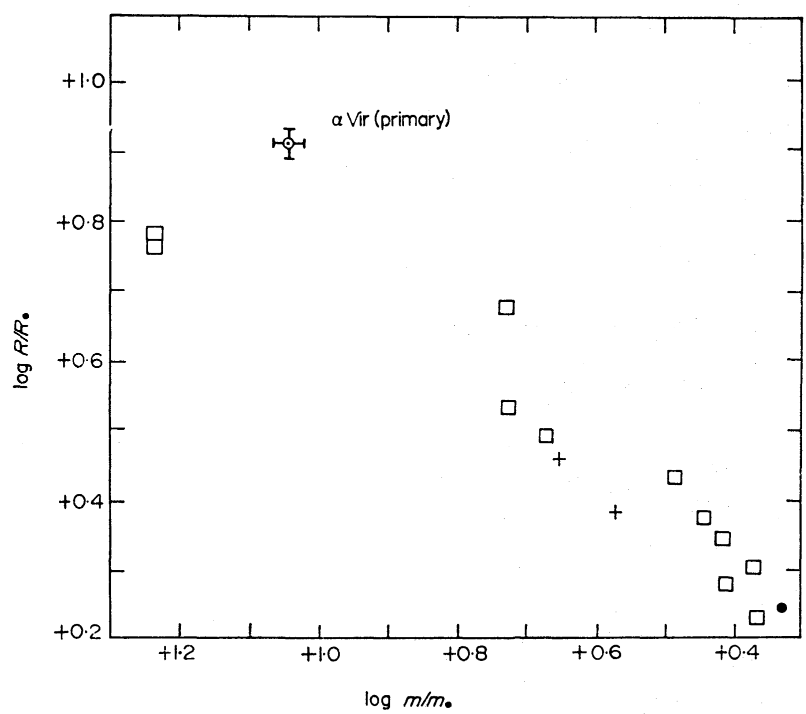

FIG. 4. *The empirical mass–radius relation for early-type stars.* □—*eclipsing binary data listed by Popper* (**30**); +—*CO Lac* (*Smak* (**29**)); ●—*α CMa* (*see text*).

and the radius from Hanbury Brown *et al.* (**3**). The data include only main-sequence components and it can be seen that the primary of α Vir lies above the mean relationship suggesting that it has evolved away from the main-sequence. The position of the primary of α Vir in Fig. 3 is consistent with this conclusion.

The spectral type of the primary of α Vir has been classified as probably B2V by Struve *et al.* (**9**), B1V by Morgan, Code & Whitford (**31**) and, more recently, as B1IV by Lesh (**32**). According to Johnson & Iriarte (**33**) the absolute magnitudes of types B1V and B1IV are $M_V = -3{\cdot}6$ and $-4{\cdot}1$, and of types B2V and B2IV are $M_V = -2{\cdot}5$ and $-3{\cdot}3$. Thus our value of $-3{\cdot}5 \pm 0{\cdot}1$ is consistent with a spectral classification between B1 and B2. Our value for the mass of the primary is consistent with this classification. We have already noted that the point for the primary of α Vir lies above the mean relationship for main-sequence components in the mass–radius diagram (Fig. 4) and we conclude that our results are consistent with a spectral classification B1·5 IV–V.

Support for this conclusion is given by the recent observation by Shobbrook *et al.* (**14**) that the primary of α Vir is a β Cepheid with a period of about 4 hr. It is also interesting to note that our value for the absolute magnitude ($-3\cdot5\pm0\cdot1$) agrees well with the period–luminosity law for β Cepheids found by Leung (**34**).

The only published spectral classification of the secondary component of α Vir appears to be that by Struve *et al.* (**9**) who noted that it is probably B3V, but may be as late as B7V. Our values for the mass ($6\cdot8\pm0\cdot7m_\odot$) and absolute magnitude ($M_{V_2} = -1\cdot5\pm0\cdot2$) are consistent with a classification B3V.

Finally, we must note that, with the parameters in Table III, α Vir may show shallow grazing eclipses. In a rough analysis of this question we have assumed that the primary is flattened at the poles by 4 per cent, due to rotation and mutual distortion, and that both components are limb-darkened with $U_{4430} = 0\cdot4$. Then, with the parameters shown in Table III, we find a grazing eclipse with a depth of approximately 1 ± 1 per cent, where the uncertainty in our estimate is largely due to the uncertainty in the inclination. Unfortunately, the observational evidence for eclipses is complicated by the β Cepheid light variations of the primary and by the mutual distortion of the two stars. According to Shobbrook *et al.* (**14**), after allowing for these complex effects, there is no residual positive evidence for eclipses and it is unlikely that they exceed 0·5 per cent. Since the depth of a grazing eclipse is critically dependent on so many factors, including our assumptions about limb-darkening, polar flattening and the angular size of the secondary, it is not worth while attempting to refine our parameters of α Vir until more positive evidence from the light curve is available.

5. CONCLUSION

The results presented above demonstrate that all the principal parameters of a double-lined, non-eclipsing, spectroscopic binary star, *including the distance*, can be found by combining observations made with an intensity interferometer with conventional spectroscopic and photometric data. It is of great interest to note, firstly, that the method gives a distance which is independent of interstellar extinction and of spectroscopic criteria of luminosity, and secondly, that it yields the inclination and hence the masses of the two stars.

In conclusion, this preliminary experiment, together with our observations of γ^2 Vel (**4**) demonstrate the potential value of a high resolution interferometer applied to the study of close binary stars. Given an instrument of greater sensitivity than the existing interferometer it would be possible to establish reasonably precise distances to many binary stars well beyond the useful limits of trigonometrical parallaxes and to extend our meagre knowledge of the masses, radii and absolute luminosities of hot stars.

ACKNOWLEDGMENTS

We are grateful to Professor D. M. Popper for his continued interest in the Narrabri programme and for his valuable advice.

The programme of the interferometer has been supported by the Air Force Office of Scientific Research (Office of Aerospace Research) of the United States Air Force under Grant (AF-AFOSR-68-1560), the Australian Research Grants Committee, the Research Grant Committee of the University of Sydney and the Science Foundation for Physics within the University of Sydney. We thank Professor H. Messel for his support.

Cornell–Sydney Astronomy Centre, School of Physics, University of Sydney

REFERENCES

(1) Brown, R. Hanbury, Davis J. & Allen, L. R., 1967. *Mon. Not. R. astr. Soc.*, **137**, 375.
(2) Brown, R. Hanbury & Browne, A., 1966. *Phillips Tech. Rev.*, **27**, 141.
(3) Brown, R. Hanbury, Davis, J., Allen, L. R. & Rome, J. M., 1967. *Mon. Not. R. astr. Soc.*, **137**, 393.
(4) Brown, R. Hanbury, Davis J., Herbison-Evans, D. & Allen, L. R., 1970. *Mon. Not. R. astr. Soc.*, **148**, 103.
(5) Michelson, A. A., 1920. *Astrophys. J.*, **51**, 257.
(6) Anderson, J. A., 1920. *Astrophys. J.*, **51**, 263.
(7) Merrill, P. W., 1922. *Astrophys. J.*, **56**, 40.
(8) Struve, O. & Ebbighausen, E., 1934. *Astrophys. J.*, **80**, 365.
(9) Struve, O., Sahade, J., Huang, S-S. & Zebergs, V., 1958. *Astrophys. J.*, **128**, 310.
(10) Vogel, H. C., 1892. *Publ. Potsdam Obs.*, **7**, 127.
(11) Baker, R. H., 1910. *Publ. Allegheny Obs.*, **1**, 65.
(12) Herbison-Evans, D. & Cramer, N., 1969. *Proc. astr. Soc. Austr.*, **1**, 205.
(13) Nelder, J. A. & Mead, R., 1965. *Computer Journal*, **7**, 308.
(14) Shobbrook, R. R., Herbison-Evans, D., Johnston, I. D. & Lomb, N. R., 1969. *Mon. Not. R. astr. Soc.*, **145**, 131.
(15) Twiss, R. Q., 1969. *Optica Acta.*, **16**, 423.
(16) Chen, K-Y, & Rhein, W. J., 1969. *Publ. astr. Soc. Pacific*, **81**, 387.
(17) Code, A. D., 1960. *Stellar Atmospheres*, p. 50, ed. J. L. Greenstein, University of Chicago Press.
(18) Oke, J. B. & Schild, R. E., 1970. *Astrophys. J.*, **161**, 1015.
(19) Davis, J. & Webb, R. J., 1970. *Astrophys. J.*, **159**, 551.
(20) Johnson, H. L., Mitchell, R. I., Iriarte, B. & Wiśniewski, W. Z., 1966. *Commun. lunar planet. Lab.*, **4**, 99.
(21) Struve, O., 1930. *Astrophys. J.*, **72**, 1.
(22) Petrie, R. M., 1948. *Publ. Dom. astrophys. Obs.*, **8**, 319.
(23) Johnson, H. L., 1966. *A. Rev. Astr. Astrophys.*, **4**, 193.
(24) Bradley, P. T. & Morton, D. C., 1969. *Astrophys. J.*, **156**, 687.
(25) Van Citters, G. W. & Morton, D. C., 1970. *Astrophys. J.*, **161**, 695.
(26) Labs, D. & Neckel, H., 1968. *Z. Astrophys.*, **69**, 1.
(27) Jenkins, L. F., 1963. *Supplement to the General Catalogue of Trigonometric Stellar Parallaxes*, p. 10, Yale University Observatory.
(28) Harris, D. L., Strand, K. AA. & Worley, C. E., 1963. *Basic Astronomical Data*, p. 287, ed. K. AA. Strand, University of Chicago Press.
(29) Smak, J., 1967. *Acta Astron.*, **17**, 245.
(30) Popper, D. M., 1967. *A. Rev. Astr. Astrophys.*, **5**, 85.
(31) Morgan, W. W., Code, A. D. & Whitford, A. E., 1955. *Astrophys. J. Suppl.*, **2**, 41.
(32) Lesh, J. R., 1969. *Astrophys. J. Suppl.*, **16**, 371.
(33) Johnson, H. L. & Iriarte, B., 1958. *Lowell Obs. Bull.*, **4**, 47.
(34) Leung, Kam-Ching, 1967. *Astrophys. J.*, **150**, 223.